

A MATHEMATICAL SIMULATION OF CONDUCTED RESPONSES IN
MICROVASCULAR NETWORKS

By

MONICA RENEE KAPP

A Thesis Submitted to The Honors College

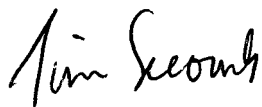
In Partial Fulfillment of the Bachelor's degree
With Honors in

Mathematics

THE UNIVERSITY OF ARIZONA

May 2009

Approved by:



Timothy W. Secomb
Department of Mathematics

A mathematical simulation of conducted responses in microvascular networks

Monica Kapp under the guidance of T.W. Secomb

ABSTRACT

In the present study, we investigated conducted responses (CR) that occur within the blood vessel walls. Two possible methods for transmission of the signal along the endothelium are active or passive. Based on the available body of knowledge, we formulated two mathematical models that simulate these transmission methods. Both models assume that the CR travels along a series of coupled endothelial cells. Our first model describes the behavior of CR based on passive spread of the signal. This model shows that a passive signal decays rapidly in a distance of about 2 mm. Since the average distance that a CR needs to be able to travel is approximately 1cm, passive spread of the signal is inadequate to describe the behavior of CR that have been observed in vivo. The second model simulates the transmission of a Ca^{2+} wave based on the involvement of a regenerative mechanism. Under the given assumptions this model shows that a regenerative mechanism allows the Ca^{2+} wave to travel distances that exceed 1cm, thereby making it a plausible transmission mechanism for a CR.

INTRODUCTION

The vascular system is a dynamic structure that is capable of accommodating variation in blood flow (5, 7, 8, 9, 10). The volume of blood that passes through a

capillary bed is dictated by the diameter of the upstream arteries and arterioles that feed it (7, 8, 9, 10). The rate of blood flow that is needed in the capillaries changes over time. When these changes occur, information needs to be sent upstream to the feeding arterioles and arteries so that their diameters are adjusted accordingly. The diameters of the feeding arteries and arterioles are adjusted by constriction or relaxation of the smooth muscle cell layer within the vessel wall. These adjustments are based on environmental signals that are detected mainly by the endothelium. The endothelium responds to both chemical and physical stimuli. The specific type of stimulus dictates whether vasoconstriction or vasodilatation occurs (12, 14).

Environmental information can be transferred upstream or downstream from the detection site via conducted responses (5, 8, 11, 1, 3, 4). Although conducted responses are most often observed on the arterial side of vascular networks, they have been shown to occur in the venules as well (3). The two known mechanisms by which signals travel are Ca^{2+} waves and membrane potential changes (4, 13, 2, 12). Our first model represents a change in membrane potential due to passive spread of current. In the second model, which depicts a regenerating signal, we considered Ca^{2+} waves dynamics.

A Ca^{2+} wave is triggered when a stimulus induces the release of Ca^{2+} from internal stores within the sarcoplasmic reticulum into the cytosol. The increase cytosolic Ca^{2+} concentration induces further release of Ca^{2+} , thereby creating a positive feedback loop. This process is known as calcium-induced-calcium-release (CICR). In this model of a CR, information is transferred by the propagation of the Ca^{2+} from one cell to the next through gap junctions. Diffusion of the Ca^{2+} from endothelial cells into smooth muscle cells through myoendothelial gap junctions can induce relaxation or constriction of the

smooth muscle cell layer (12, 13, 14). Despite the coupling between the endothelium and the smooth muscle cell layer, it has been shown that the Ca^{2+} waves of the conducted response propagates along the endothelium of blood vessels but not the smooth muscle cell layer (12). This is reasonable, since the endothelial cells lie parallel to the vessel axis, while the smooth muscle cells are circumferential oriented (see Fig. 1). This structural arrangement allows the Ca^{2+} waves to propagate at a much faster rate along the endothelium then along the smooth muscle cell layer.

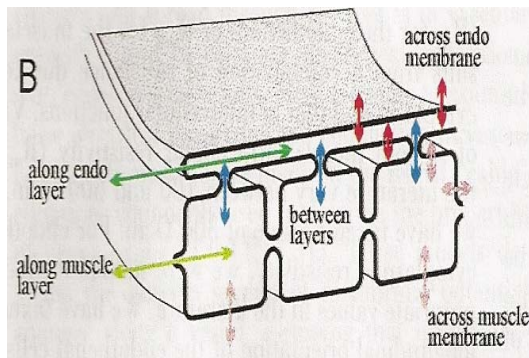


Fig. 1. Structural orientation of the smooth muscle cells and the endothelial cells within blood vessel walls. Arrows indicate coupling between cells.

Due to CICR, a single cell produces a spike in $[\text{Ca}^{2+}]_{\text{cyt}}$ in response to a small increase in the $[\text{Ca}^{2+}]_{\text{cyt}}$. After reaching its peak, the $[\text{Ca}^{2+}]_{\text{cyt}}$ returns to the baseline concentration as the Ca^{2+} stores are refilled.

If cells are coupled by gap junctions then as the $[\text{Ca}^{2+}]_{\text{cyt}}$ spikes in one cell, the increased $[\text{Ca}^{2+}]_{\text{cyt}}$ causes a flux of Ca^{2+} from the first

cell to the next cell, possibly triggering a spike in the second cell.

Based on the given information, we considered the transmission of a CR along a string of coupled endothelial cells with the structural arrangement as shown in Fig. 2a. For the sake of simplicity our models assume that each EC is coupled only to two adjacent cells at opposite sides of the EC. This is a simpler coupling structure than the true coupling of EC in vessel walls. Fig. 2b shows the true structural orientation of EC in a vessel wall. Another simplification of our model is that we only considered coupling between EC, and not coupling between EC and SMC.

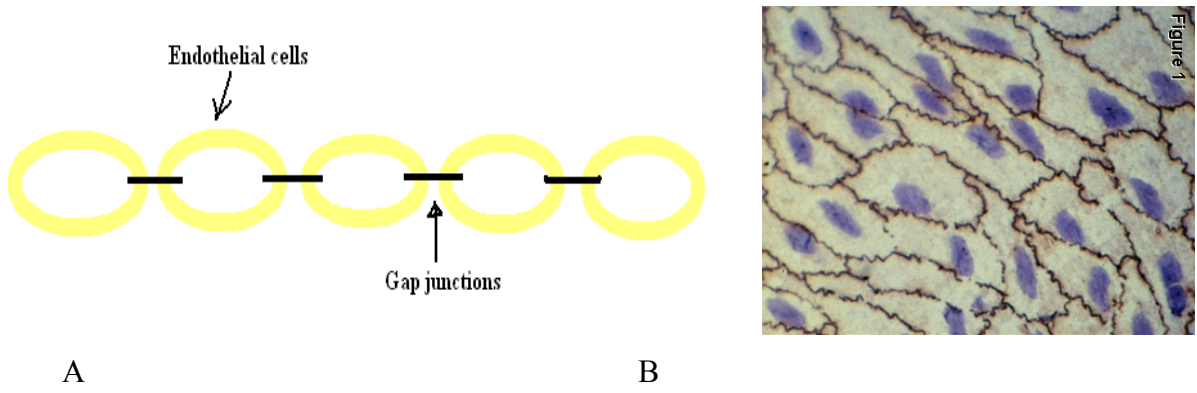


Fig 2. 2a. Schematic drawing of our assumed coupling structure. 2b. true coupling structure for EC seen in vivo.

Based on the above assumptions we constructed two mathematical models to simulate conducted responses within the vascular network. Model 1 is a simulation of passive spread of current, while model 2 depicts active spread via a regenerative mechanism. Model 2 is based on the two pool model of Ca^{2+} oscillations as described by Keener and Sneyd in their book (6). Both models were used to make predictions about the behavior of conducted responses. The predictions were compared with the observed behavior.

METHODS

Model 1: passive spread

Propagation of conducted responses along a string of coupled endothelial cells was modeled as an electrical current along a wire. By Ohm's Law, the current satisfies

$$i(x) = -\frac{1}{r_i} \frac{dV_i(x)}{dx} \quad (1)$$

where $i(x)$ is the current, $V_i(x)$ is the internal voltage, and r_i is the resistance per unit length. Based on conservation of current and the principles of Ohm's Law we have,

$$\frac{di(x)}{dx} = -i_m(x) = [V_e - V_i(x)]g_m \quad (2)$$

where $i_m(x)$ is the amount of the signal which transverses the cell membrane, V_e is the external voltage, and g_m is the conductance per unit length. Combining equations (1) and (2) gives,

$$-\frac{1}{r_i} \frac{dV_i^2(x)}{dx} = [V_e - V_i(x)]g_m \quad (3)$$

Boundary conditions are, $V_A = V_i(0)$ and $V_B = V_i(L)$, where V_A represents the voltage at the signal initiation site and V_B represents the voltage at a given distance from the signal initiation site. The general solution of equation (3) can be written in the form:

$$V_i(x) = a \sinh(\lambda x) + b \sinh[\lambda(L - x)] + V_e \quad (4)$$

where $\lambda = \sqrt{r_i g_m}$. Applying the boundary conditions we find

$$a = \frac{V_B - V_e}{\sinh(\sqrt{r_i g_m} L)} \quad b = \frac{V_A - V_e}{\sinh(\sqrt{r_i g_m} L)} \quad (5)$$

and so the particular solution for $V_i(x)$ is:

$$V_i(x) = \frac{1}{\sinh(\sqrt{r_i g_m} L)} \left[(V_B - V_e) \sinh(\sqrt{r_i g_m} x) + (V_A - V_e) \sinh(\sqrt{r_i g_m} (L - x)) \right] + V_e \quad (6)$$

Model 2: active spread via Ca^{2+} waves

Fig. 3. shows a schematic drawing of the two pool model used to describe Ca^{2+} oscillations.

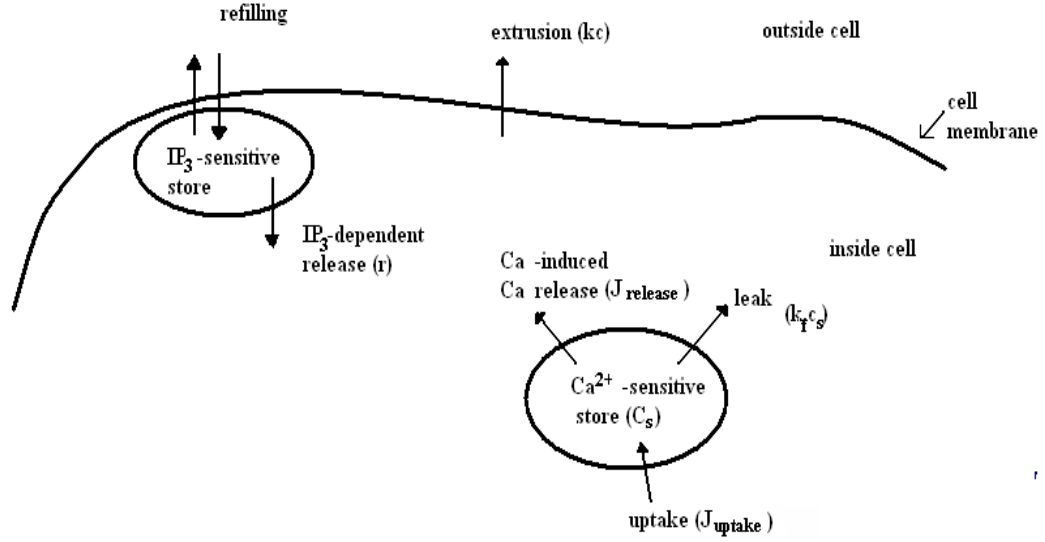


Fig. 3. two pool model of Ca^{2+} oscillations.

As the foundation of our second model, we used the following equations (6).

$$\frac{dc}{dt} = r - kc - \tilde{f}(c, c_s) \quad (7)$$

$$\frac{dc_s}{dt} = \tilde{f}(c, c_s) \quad (8)$$

$$\tilde{f}(c, c_s) = J_{\text{uptake}} - J_{\text{release}} - k_f c_s \quad (9)$$

where c is $[\text{Ca}^{2+}]_{\text{cyt}}$, c_s is $[\text{Ca}^{2+}]_{\text{store}}$, r is the constant rate at which Ca^{2+} is released from the IP_3 -dependent store, kc is the rate that Ca^{2+} is pumped out of the cytosol, $k_f c_s$ is the rate that Ca^{2+} leaks out of the internal Ca^{2+} store, and

$$J_{\text{uptake}} = \frac{V_1 c^n}{K_1^n + c^n} ,$$

$$J_{\text{release}} = \left(\frac{V_2 c_s^m}{K_2^m + c_s^m} \right) \left(\frac{c^p}{K_3^p + c^p} \right) \quad (\text{See Fig. 3})$$

We assumed that the concentrations in each pool are expressed as amount per total cell volume. Equations (7), (8), and (9) were non-dimensionalized as follows (6):

$$u_q = \frac{c}{K_1}, \tau = tk, v_q = \frac{c_s}{K_2}, \alpha = \frac{K_3}{K_1}, \beta = \frac{V_1}{V_2}, \gamma = \frac{K_2}{K_1}, \delta = \frac{k_f K_2}{V_2}, \mu = \frac{r}{kK_1}, \& \varepsilon = \frac{kK_2}{V_2}$$

where the subscript q is the cell number. The resulting non-dimensional equations describing calcium dynamics in cell q are:

$$\frac{du_q}{d\tau} = \mu - u_q - \frac{\gamma}{\varepsilon} f(u_q, v_q) \quad (11)$$

$$\frac{dv_q}{d\tau} = \frac{1}{\varepsilon} f(u_q, v_q) \quad (12)$$

$$f(u_q, v_q) = \beta \left(\frac{u_q^n}{u_q^n + 1} \right) - \left(\frac{v_q^m}{v_q^m + 1} \right) \left(\frac{u_q^p}{\alpha^p + u_q^p} \right) - \delta v_q \quad (13)$$

To account for intercellular transmission of the Ca^{2+} wave we added a term to equation (11).

$$\frac{du_q}{d\tau} = \mu - u_q - \frac{\gamma}{\varepsilon} f(u_q, v_q) - k_{\text{cond}}(u_q - u_{q-1}) \quad (14)$$

where k_{cond} is the permeability of the gap junction connecting the cytosol of adjacent cells. Equations (12) and (14) were solved using the MATLAB program ode15s, and plotted using MATLAB.

RESULTS

Model 1

To test model 1, we choose the following set of parameters:

segment length = 1 cm

$$V_e = 0\text{mV}$$

$$V_i(0) = V_A = -50\text{mV}$$

$$g_m = 8 \times 10^{-8} \Omega^{-1} \text{ cm}^{-1}$$

$$V_i(1) = V_B = 0\text{mV}$$

$$r_i = 1.2 \times 10^9 \Omega^1 \text{ cm}^{-1}$$

These model parameters are based on values reported by Crane (4). Based on the above values we obtained, the potential in mV is given by

$$V_i(x) = \frac{-50 \sinh[4\sqrt{6}(1-x)]}{\sinh(4\sqrt{6})} \quad (15)$$

where x is the position along the vessel in cm. The graph of equation (15) is shown in Fig. 4. The exponential decay of the signal is consistent with a passive transport mechanism.

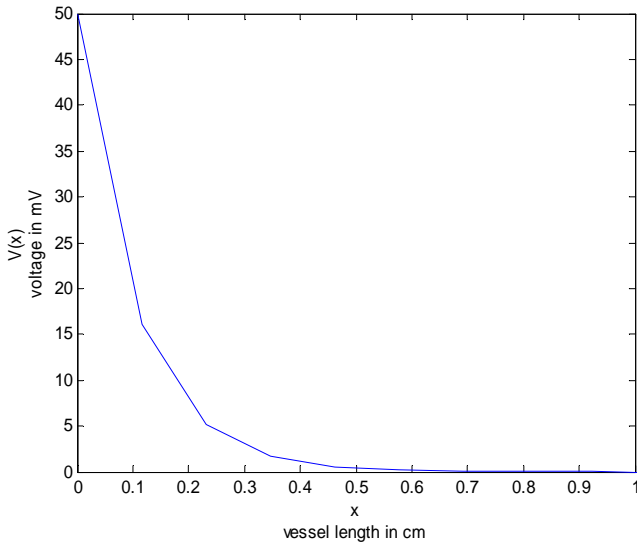


Fig. 4. model of the exponential decay of a signal transmitted by passive transport. This model is based on a 1cm long vessel segment.

Model 2

First we considered the transient response to a small spike in $[Ca^{2+}]_i$ in a single endothelial cell. Using the following set of parameters we obtained the graph shown in Fig 5.

$$\begin{array}{ll} \alpha = 0.9; & \mu_{\text{pulse}} = 0.1; \\ \beta = 0.13; & \epsilon = 0.04; \\ \gamma = 2; & m = 2; \\ \delta = 0.004; & n = 2; \\ \mu = 0.3; & p = 4; \end{array}$$

Next we examined the effects of coupling between adjacent cells on the transient cellular response to a small $[Ca^{2+}]_{\text{cyt}}$ spike. For this we used equations (12), (13), and (14).

The parameters used are the same as those used in the single cell trial, with $k_{\text{cond}} = 0.04$. The results are shown in Fig 6. To calculate the wave propagation rate we used the average interval between times at which successive cells start the Ca^{2+} spike.

This gave a rate of $\sim 100 \mu\text{m s}^{-1}$. Fig. 7 shows the dependence of the wave propagation rate on k_{cond} .

The degree of coupling dictates both the distance the Ca^{2+} wave will travel and its propagation rate. If the coupling between cells is too low then a $[\text{Ca}^{2+}]_{\text{cyt}}$ spike in one cell will not induce a spike in coupled cells because not enough Ca^{2+} will be transferred from one cell

to the next to reach the threshold level in the coupled cell. If the degree of coupling between cells is too great then even a small $[\text{Ca}^{2+}]_{\text{cyt}}$ increase in the first cell will diffuse to adjacent cells before the threshold level of CICR is reached in the first cell. In this case no $[\text{Ca}^{2+}]_{\text{cyt}}$ spike is observed. There is a range in the degree of coupling in which a wave is observed propagating from one cell to the next. Faster wave propagation rate are

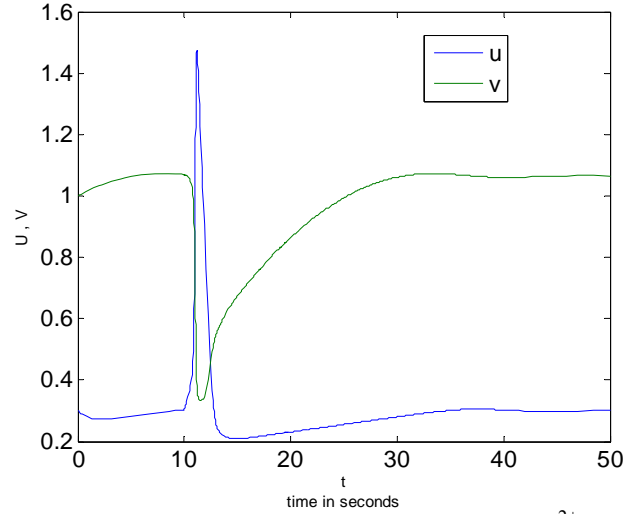


Fig. 5. Transient response to a change of $[\text{Ca}^{2+}]$ in a single EC.

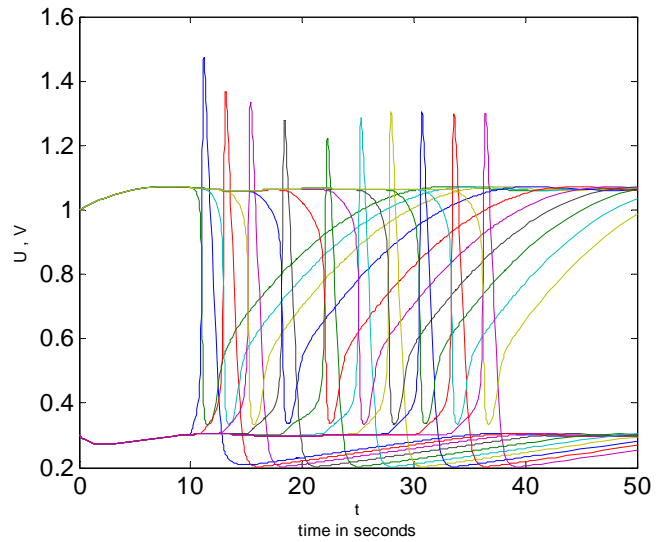


Fig. 6. transient response to the change of $[\text{Ca}^{2+}]$ in a multiple, coupled EC.

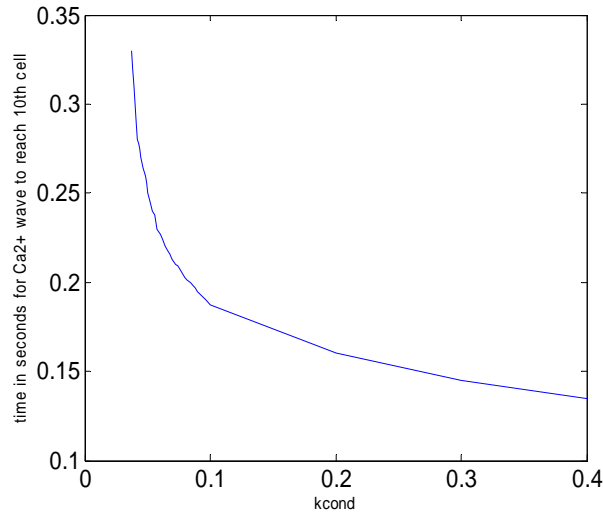


Fig. 7. dependence of Ca^{2+} wave propagation rate on k_{cond} .

observed at higher the degree of coupling.

DISCUSSION

The average distance that a conducted response must travel from a capillary to an upstream arteriole is approximately 1 cm. Our passive spread model shows that after approximately 2

mm, 90% of the signal is lost. Although propagation of conducted responses was originally assumed to occur via a passive spread of the information (11), our model shows that passive spread of the conducted response is inadequate to describe their behavior. Our findings are consistent with those of Berg et al. (1).

When considering Ca^{2+} dynamics one would expect a time lag between the time when the Ca^{2+} wave enters the cytosol of a cell until it diffuses across the length of the cell and enters the cytosol of the next cell. Our model neglects this time lag and assumes that Ca^{2+} is instantaneously, uniformly diffused throughout the cytosol as soon as it enters the cytosol. Therefore our model is expected to overestimate the wave propagation velocity. However in reality EC are coupled on all sides to multiple cells, which may increase the propagation rate from that expected under our assumed coupling structure. This may compensates somewhat for the error introduced by this assumption.

The degree of coupling between adjacent EC dictates the rate at which the Ca^{2+} wave travels from one cell to the next. Faster wave propagation rates are observed at

higher degrees of coupling. If there is not enough coupling between cells then no Ca^{2+} wave is observed. At low degrees of coupling, a wave may travel from the first cell to as many as four cells away before it dies out. We found that the critical conductance at which the wave is able to transverse the entire length of ten coupled cells is $k_{\text{cond}} = 0.0375$. Using this conductance rate, and taking individual endothelial cell width to be $20\mu\text{m}$, our model indicates the Ca^{2+} wave travels at approximately $100\mu\text{m s}^{-1}$. This is approximately the same speed that Uhrenholt et al (12) measured Ca^{2+} waves traveling in the endothelium.

In our model, k_{cond} has units of number of Ca^{2+} ions per unit time that pass through the gap junction. We were therefore unable to compare our k_{cond} values to the conductance values that have been measured in vivo, because in vivo conductance is measured in $\Omega^{-1} \text{cm}^{-1}$. For this reason it is unclear if our k_{cond} value is consistent with the conductance measured in vivo.

Producing a workable model that simulates conducted response in vascular networks will provide insights into the maintenance and growth mechanisms that regulate vascular structure. Many diseases either affect the vascular system or are affected by its structure. For example tumor blood vessels have chaotic and inefficient network structures. One theory is that the number of functional gap junctions is insufficient to achieve efficient intracellular communication. This lack of communication may lead to the chaotic vessel structure seen in tumors. Better understanding of how CR function in normal tissue may help us to understand and control vascular properties and other types of disease.

REFERENCES

1. **Berg BR, Cohen KD, and Sarelius IH.** Direct coupling between blood flow and metabolism at the capillary level in striated muscle. *Am. J. Physiol* 272: H2693-H2700, 1997.
2. **Blatter LA, and Wier WG.** Agonist-induced $[Ca^{2+}]_i$ waves and Ca^{2+} -induced Ca^{2+} release in mammalian vascular smooth muscle cells. *Am. J. Physiol Heart Cir Physiol* 263: H576-H586, 1992.
3. **Collins DM, McCullough WT, and Ellsworth ML.** Conducted vascular responses: communication across the capillary bed. *Microvascular Research* 56: 43-53, 1998.
4. **Crane GJ, Hines ML, and Neild TO.** Simulating the spread of membrane potential change in arteriolar networks. *Microcirculation* 8: 33-43, 2001.
5. **Dora KA, Damon DN, and Duling BR.** Microvascular dilation in response to occlusion: a coordination role for conducted vasomotor responses. *Am. J. Physiol Heart Cir Physiol* 279: H279-H284, 2000.
6. **Keener J, and Sneyd, J.** *Mathematical Physiology*. Springer. 2001 p.160-166.
7. **Pries AR, Reglin R, and Secomb TW.** Remodeling of blood vessels responses of diameter and wall thickness to hemodynamic and metabolic stimuli *Hypertension* 46: 725-731, 2005.
8. **Pries AR, and Secomb TW.** Control of blood vessel structure: insights from theoretical models. *Am. J. Physiol Heart Cir Physiol* 288: H1010-H1015, 2005.
9. **Pries AR, and Secomb TW.** Structural adaptation of microvascular networks and development of hypertension. *Microcirculation* 9: 305-314, 2002.
10. **Pries AR, Secomb TW, and Gaehtgens P.** Structural adaptation and stability of microvascular networks: theory and simulations. *Am. J. Physiol Heart Cir Physiol* 275: H349-H360, 1998.
11. **Secomb TW, and Pries AR.** Information transfer in microvascular networks. *Microcirculation* 9: 377-387, 2002.
12. **Uhrenholt TR, Domeier TL, and Segal SS.** Propagation of calcium waves along endothelium of hamster feed arteries. *Am. J. Physiol Heart Cir Physiol* 292: H1634-H1640, 2007.
13. **Yasuaki Y, and Duling BR.** Participation of intracellular Ca^{2+} stores in arteriolar conducted responses. *Am. J. Physiol Heart Cir Physiol* 285: H65-H73, 2003.
14. **Zacharia J, Zhang J, and Wier WG.** Ca^{2+} signaling in mouse mesenteric small arteries: myogenic tone and adrenergic vasoconstriction. *Am. J. Physiol Heart Cir Physiol* 292: H1523-H1532, 2007.

STATEMENT BY AUTHOR

I hereby grant to the University of Arizona Library the nonexclusive worldwide right to reproduce and distribute my thesis and abstract (herein, the "licensed materials"), in whole or in part, in any and all media of distribution and in any format in existence now or developed in the future. I represent and warrant to the University of Arizona that the licensed materials are my original work, that I am the sole owner of all rights in and to the licensed materials, and that none of the licensed materials infringe or violate the rights of others. I further represent that I have obtained all necessary rights to permit the University of Arizona Library to reproduce and distribute any nonpublic third party software necessary to access, display, run, or print my thesis. I acknowledge that University of Arizona Library may elect not to distribute my thesis in digital format if, in its reasonable judgment, it believes all such rights have not been secured.

SIGNED: Monica R. Kopp